Thermal Model and Analysis of Wound Rotor Induction Machine

Aldo Boglietti[1] *Fellow member IEEE,* Andrea Cavagnino[1] *Senior member IEEE* ,
Mircea Popescu[2] *Senior member IEEE,* David Staton[2] *Member IEEE*
1) Politecnico di Torino, Dipartimento Energia, Italy
2) Motor Design Ltd., UK

***Abstract* -This paper presents a simplified thermal model for a wound rotor induction machine. The thermal model is based on lumped parameters and the analytical equations for their computation are provided in the paper. The procedures for the thermal model set up have been discussed and validated on a 3.8 hp wound rotor machine, comparing the predicted and measured temperature. Due to the complex cooling system adopted for the tested machine, the techniques for its modeling have also been reported and discussed. The accuracy of the proposed thermal model with a less than 7 percent incidence of error is considered more than reasonable, taking into account the complexity of the system under analysis.**

Keywords: wound rotor induction motor, thermal analysis, thermal model, wind generators, forced convection.

LIST OF SYMBOLS

$D_{i\text{-}St}$	Inner stator diameter
$D_{e\text{-}Rot\text{-}Yoke}$	Outer rotor diameter
$D_{i\text{-}Rot\text{-}Yoke}$	Inner rotor diameter
D_{s_out}	Outer stator lamination diameter
D_{FR_i}	Inner frame diameter
d_{eq}	Equivalent diameter for annular section duct
L_{st}	Stator stack length
L_{rot}	Rotor stack length
$N_{S\text{-}rot}$	Rotor slot number
$P_{erS\text{-}Rot}$	Rotor slot perimeter
t_{eq}	Thickness of the equivalent slot insulation
$S_{Co\text{-}rot}$	Rotor copper area in a rotor slot
$S_{S\text{-}rot}$	Rotor slot area
h_{ai}	Thermal convection coefficient
h_{AG}	Air thermal conductivity
k_{Ir}	Iron thermal conductivity
h_m	Average forced convection coefficient
ω_{mec}	rotor mechanical speed
K_f	Slot filling factor
A_{slot}	Slot area
L_{core}	Machine length
k_{air}	air thermal conductivity
Nu	Nusselt number
Re	Reynolds number
Pr	Prandtl number
v_{air}	Air speed
μ_{air}	Air viscosity
δ_{air}	Air density
c_s	Air specific heat
T_{ir}	iron temperature
T_m	Average cooling air temperature
T_{amb}	Ambient temperature
$T_{ex\text{-}ec}$	Air temperature at the exhaust end-cap
$P_{FR\text{-}AMB}$	Natural convection heat transfer coefficient between the frame and the ambient
$P_{Forced\text{-}Air}$	Cooling power due to forced air
P_{Losses}	Machine losses

I. INTRODUCTION

In the last 20 years, wind energy has been the fastest growing energy technology. In particular, wind energy is the only power generation technology that can promise the necessary CO_2 emission limitations in the critical period of the next 10 years. The 120.8 GW of global wind potential capacity will produce 260 TWh and save 158 million tons of CO_2 every year.
From 2005 to 2008 the installed wind capacity doubled and the trend seems to continue, as shown in Fig. 1 [1]. As shown in Fig.2, the cumulative capacity is growing worldwide and in 2008 around 44 % of this had been installed in Europe (57380 MW), a further 21% in North America (25170 MW) and 18% in Asia and the Pacific (21855 MW). The countries with the largest installed wind power capacity in Europe are Germany (23903 MW), Denmark (3180 MW) and Spain (16754 MW), countries which thus have 36% of the total installed capacity worldwide. Wind energy technology itself has moved very fast whilst revisiting old technologies such as wound-rotor induction machine "WRIM" with two power electronics converters connected back-to-back in the rotor circuit [2]. This solution makes up the majority in the wind generators world market. The other generator topologies in competition with the WRIM are the permanent magnet synchronous generator and the squirrel-cage induction generator both with full-scale frequency converters in the stator circuit [3].
In wind generators the WRIM presents several advantages:

- The capability to control reactive power and to decouple active and reactive power control by independent control of the rotor current.
- The machine can also be magnetized from the rotor side. As a consequence, it is not necessary to get the magnetizing current directly from the power grid.
- The machine is capable of generating reactive power that can be delivered to the stator by the grid-side converter.
- In the presence of weak grids with voltage fluctuation it can produce or absorb reactive power, allowing the grid voltage control.

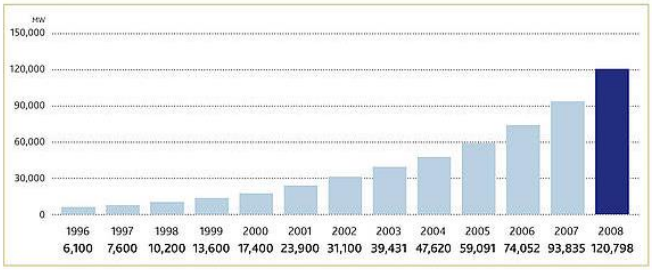

Fig.1: Global cumulative installed wind generators capacity in the period 1996- 2008 [1].

- The converter power size is not related to the generator total power but is dependent upon the selected speed range. Put simply, the converter size is dependent on the slip power value. A converter size of around 25% of the generator total power is usual adopted, based on economic optimizations, investment costs and efficiency.

For the reasons previously discussed, during the last decade, there has been a renewed interest in the theory, modeling, control and technologies related to WRIM. Among these topics the thermal analysis assumes a relevant role due to the presence of windings in the rotor.

In a traditional squirrel cage induction motor, the thermal behavior of the rotor does not represent a crucial aspect. In fact, aluminum die cast cages can tolerate temperatures higher than the stator winding where the insulation system (wire enamel, liner, impregnation etc.) imposes strict temperature limitations. On the contrary, in a WRIM both stator and rotor are subordinated to the temperature limitation of the insulation system. This fact increases the complexity of thermal analysis of a WRIM and a correct thermal representation of the stator and rotor tooth zones is mandatory.

In the past, the authors have dealt with the problem of obtaining simple but accurate enough thermal models of squirrel cage induction motors based on lumped parameters, with particular attention to the winding structure [4]-[9]. In the same period, other authors have given their contribution to these important topics [11]-[13].

In this paper the authors, starting from the simplified thermal model for a self-cooled industrial induction motor discussed in [7], propose a thermal model suitable for WRIM. This thermal model, based on lumped parameters, is deeply discussed and its validity is verified by experimental tests. A complete experimental procedure for the thermal model set up is included, providing interesting and useful information to researchers interested on this topic.

II.WRIM THERMAL MODEL

The proposed WRIM thermal model is an evolution of the thermal model proposed in 2003 for TEFC "Total enclosed fan cooled" industrial induction motor [7]. The proposed thermal network is shown in Fig. 3. Hereafter the modifications introduced with respect to the original thermal model are listed and explained making reference to Fig. 3, where the new thermal parameters are drawn in gray color.

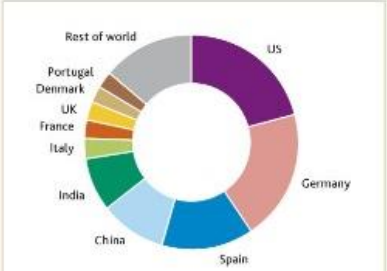

	MW	%
USA	25,170	20.8
Germany	23,903	19.8
Spain	16,754	13.9
China	12,210	10.1
India	9,645	8.0
Italy	3,736	3.1
France	3,404	2.8
UK	3,241	2.7
Denmark	3,180	2.6
Portugal	2,862	2.4
Rest of world	16,693	13.8
Total top 10	**104,104**	**86.2**
World total	**120,798**	**100.0**

Fig. 2: Top 10 total installed capacity in 2008 [1]

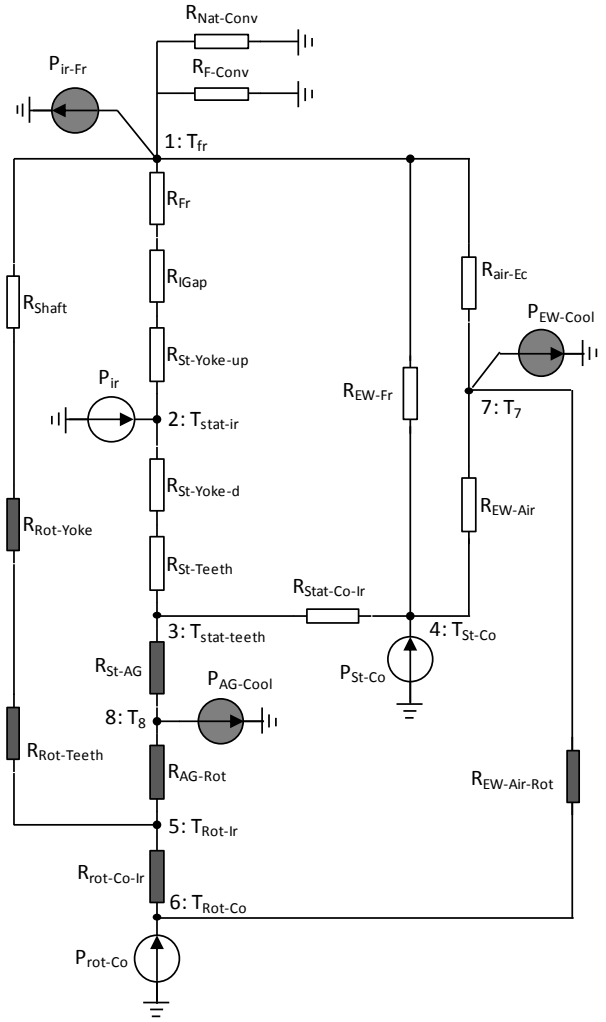

Fig.3: Proposed thermal model for WRIM.

All the other thermal parameters coming from the original thermal network are discussed in [7], where all the equations for computation of the new ones are reported in detail.

New thermal nodes:

- Node 7 represents the temperature of the air inside the end-caps [8]. This node has been added for taking into account the heat contribution coming from the rotor end-winding.
- Node 8 represents the temperature of the air inside the air gap. This node has been added for including the cooling forced convection heat transfer through the machine airgap.

New cooling sources:

- $P_{EW\text{-}Ec}$ is a heat generator for taking into account the cooling forced convection acting on the end-windings.
- $P_{AG\text{-}cool}$ is a heat generator for taking into account the cooling forced convection acting in the air-gap.
- $P_{ir\text{-}Fr}$ is a heat generator for taking into account the cooling forced convection acting on the outer surface of the stator laminations.

These cooling sources pull out heat from the system (negative heat generators) and they are required for the particular forced cooling system used in the WRIM adopted for testing the proposed thermal model. Depending upon the cooling system of the machine these heat generators can be nullified, setting their values to zero.

New thermal resistances:

$R_{Rot\text{-}Yoke}$ is the conductive thermal resistance of the rotor back iron. It is calculated by (1):

$$R_{Rot-Yoke} = \frac{1}{2\pi L_{St} \cdot k_{Ir}} \cdot \ln \frac{D_{e-Rot-Yoke}}{D_{i-Rot-Yoke}} \quad (1)$$

$R_{Rot\text{-}Teeth}$ is the conductive thermal resistance of the rotor teeth. It is calculated by (2):

$$R_{Rot-Teeth} = \frac{1}{2\pi L_{St} \cdot k_{Ir} \cdot P} \cdot \ln \frac{D_{e-Rot}}{D_{i-Rot\_Yoke}} \quad (2)$$

$R_{St\text{-}AG}$ and $R_{AG—Rot}$ are the two air-gap thermal resistances. The two resistances have the same value equal to half of the air-gap total thermal resistance. The air-gap total thermal resistance has been split in two in order to create the thermal node 8 where the heat generator $P_{AG\text{-}cool}$ is connected. Due to the narrow thickness of the air-gap and the necessity to simplify the thermal model, this heat transfer has been considered for conduction only [7]. They are calculated by (3).

$$R_{St-AG} = R_{AG-Rott} = \frac{0{,}5}{2\pi L_{St} \cdot k_{air}} \cdot ln \frac{D_{i-St}}{D_{i-St} - 2 \cdot h_{AG}} \quad (3)$$

$R_{RotCo\text{-}Ir}$ is the equivalent conductive thermal resistance between the rotor copper and the rotor lamination. It is calculated by (4):

$$R_{Rot-Co-Ir} = \frac{t_{eq}}{k_{Rot-Co-Ir} \cdot S_{T-S-Rot}} \quad (4)$$

where the inner surface of all the rotor slots $S_{T\text{-}S\text{-}Rot}$ is calculated as shown in (5)

$$S_{T-S-Rot} = n_{S-Rot} \cdot Per_{S-Rot} \cdot L_{Rot} \quad (5)$$

and t_{eq} by (6)

$$t_{eq} = \frac{S_{S-rot} - S_{Co-rot}}{Per_{S-Ro}} \cdot \quad (6)$$

$R_{EW\text{-}Ar\text{-}Rot}$ is the forced convection thermal resistance between the end-winding and the end-cap internal air. It is calculated by (7).

$$R_{EW-Air-Rot} = \frac{1}{2\pi \cdot (L_{ec} - L_{St}) \cdot D_{e-Rot} \cdot h_{ai}} \quad (7)$$

Where h_{ai} is calculated by (8) [8].

$$h_{ai} = 41{,}4 + 6{,}22 \cdot \omega_{mec} \cdot \frac{D_{e-Rot}}{2} \quad (8)$$

In thermal models of electrical machines it is important to pay attention to the equivalent thermal conductivity resistance between the copper in the slots and the lamination. This parameter is very complex to predict due to the "winding-slot" geometries and structure and the number of materials involved (copper, wire insulating enamel, slot liner, impregnation, air, etc.). In addition, this thermal resistance is strongly dependent on the impregnation process adopted by the machine manufacturer. In [7] the authors proposed an equivalent slot thermal conductivity $K_{Cu\text{-}ir}$ to be used for the computation of the thermal resistance representing the overall insulation and impregnation volume inside the slot (computed as the difference between the slot and the copper volume). On the basis of thermal tests on several induction motors, the simple equation (9) has been found and presented in [7].

$$K_{Cu-Irc} = 0.2425\, x^{-0.4269} \quad (9)$$

where $x = (1\text{-}K_f)\, A_{slot}\, L_{core}$ is the total insulation volume inside the slots. In Fig. 4 the representation of the proposed curve and the values obtained by experimental test is reported.
The use of (9) for the computation of the thermal resistances $R_{Stat\text{-}Co\text{-}Ir}$ and $R_{Rot\text{-}Co\text{-}Ir}$ has to be considered as a first attempt. As described in the next section, more accurate results can be obtained after a thermal model calibration.

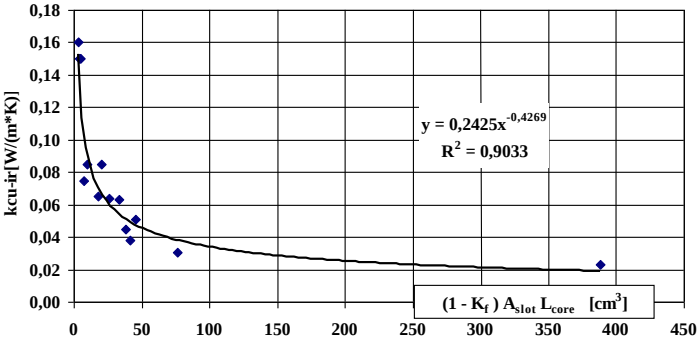

Fig. 4: Equivalent slot thermal conductivity.

Fig. 5: WRIM under test.

III. Thermal Model Set Up

The proposed thermal model has been firstly set up and subsequently validated on a wound rotor induction motor available in the laboratory (see Fig. 5), having the following nameplate data:

Rated power	3.8 hp
N poles	6
Stator rated voltage	380/200 V
Stator rated current	7/1.2 A
Stator phases	3
Rated rotor voltage	124 V
Rated rotor current	17.3 A
Rotor phases	2
Rated speed	925 rpm

As discussed in [5] and [7] the use of a thermal model is not easy because the computation of some thermal resistances is strongly dependent upon several parameters for which reliable data may be difficult to find, for example, equivalent thermal conductivity between winding and lamination, forced convection heat transfer, radiation heat transfer coefficient, interface gap between components, air cooling speed, etc. Designers with a great working experience on similar designs, using comparable manufacturing processes, can make a correct choice of such parameter values, however, these choices are generally very difficult, compromising the final results if made wrongly.

As a consequence, a preliminary set up of the thermal models, when possible, is highly recommended by the authors.

The critical thermal parameters can be estimated by means of thermal test with DC supply and the rotor still, because in this test only the stator copper losses are active and no loss contribution separation is necessary as requested with an AC supply test. During the test the DC supply current has to be reduced to 50-70% of the rated current to avoid thermal damage due to zero cooling air speed. In steady state thermal condition the adsorbed electrical power and the temperatures of the stator windings, stator core and external housing have to be measured.

With respect to industrial induction motors, WRIM has windings both in the stator and the rotor. As a consequence, the measuring methodology described in [5] has to be modified.

In fact, for a WRIM three thermal tests with DC supply are requested:

- Thermal test with DC supply of the stator winding;
- Thermal test with DC supply of the rotor winding;
- Thermal test with DC supply of both the stator and rotor windings.

In order to get accurate test results, the windings, lamination and external frame temperature have to be measured in steady state thermal conditions. If the lamination temperature measurement is not possible, this measure can be neglected losing the possibility to estimate the interface gap between lamination and external frame. Since the tests are in DC supply, the winding temperature can be easily monitored directly by the winding resistance measure, while the other temperatures can be measured using a good digital thermometer. The frame temperature can be measured as the average temperature of several points on the machine frame. The following electrical power has been used for the three tests:

- Stator supply only: 98.1 W
- Rotor supply only: 78.6 W
- Stator and rotor supply: 96.6 W (stator)- 46.5 W (rotor)

For the machine under test, the thermal steady state is reached after 7 hours. All the thermal resistances reported in Fig. 3 due to conduction heat transfer have been computed using the motor geometrical data. Since the motor is still, the thermal resistances due to the forced convection heat transfer can be neglected and removed by the thermal network. On the basis of the DC thermal tests, the following thermal quantities have been estimated:

- natural convection thermal resistance between frame and ambient;
- equivalent interface gap between lamination and motor frame;
- equivalent thermal conductivity between stator copper and stator lamination;
- equivalent thermal conduction between rotor copper and rotor lamination

In particular, the following step by step set up procedure has been adopted:

1) for the thermal test with stator DC supply a $K_{Stat\text{-}Co\text{-}Ir}$ starting value is calculated using (9) and an interface gap equal to zero is considered;
2) the natural convection resistance is calculated using (10);

$$R_{Nat-Conv} = \frac{T_{Frame} - T_{Ambient}}{P} \quad (10)$$

3) The equivalent interface gap between the stator lamination and the external frame is changed until a good match

between measured and computed stator lamination temperatures is obtained;

TABLE I
THERMAL QUANTITIES AFTER MODEL SET UP

$R_{Nat-Conv}$[K/W]	l_{ig}[mm]	$k_{St-Co-Fe}$[W/(m K)]	$k_{Rot-Co-Fe}$[W/(m K)]
0,169	0,6	0,1	0,03

4) In the same way, the coefficient $K_{Stat-Co-Ir}$ is changed until the computed temperature of the stator copper matches the measured one;
5) The obtained results have been considered for the simulation in the thermal test with rotor DC supply;
6) The $K_{Rot-Co-Ir}$ is changed until the error between the measured and computed temperature of the rotor copper is lower than a defined percentage. In the proposed study, a percentage equal to 5% has been considered a good compromise;
7) The obtained values have been adopted to simulate the thermal test with stator and rotor windings simultaneously DC supplied;
8) Finally, the values of the interface gap, $K_{Stat-Co-Ir}$,$K_{Rot-Co-Ir}$ are modified to give a good match between the predicted and measured temperature for the stator laminations, stator and rotor copper. Again, percentage errors lower than 5% have been considered acceptable for the description of the tests with DC supply.

Table I summarizes the value of the obtained quantities after the minimization procedure.
The results reported in Table I require some comments and considerations. The equivalent thermal conductivities both for the stator and rotor slots are lower than the starting values computed by (9); 0.167 for the stator slots and 0.0858 for the rotor slots respectively. This result can be justified because the machine is old (manufactured in the 1960's) and the insulation and impregnation materials are not comparable with modern ones. It is important to underline that the equivalent thermal conductivities reported in Fig. 4 were obtained on modern industrial induction motors.
The value of the equivalent interface gap is one size higher than the value presents in industrial induction motors. This difference is due to the assembly technique of the stator core inside the machine frame. Usually in industrial induction motors the stator core is thrust in the frame and the equivalent interface gap is due to the roughness of the stator core and machine frame surfaces with an average size of some hundredths of millimiters. In the machine under test the stator core is kept in position using twelve supports (one such support is shown in Fig. 6). The duct between stator core and frame is used for cooling the machine by forced air produced by a fan mounted on the rotor shaft. As a consequence, the value of the equivalent interface gap found with the thermal network set up takes into account the conduction heat paths due to the air in the duct and the twelve metallic supports.

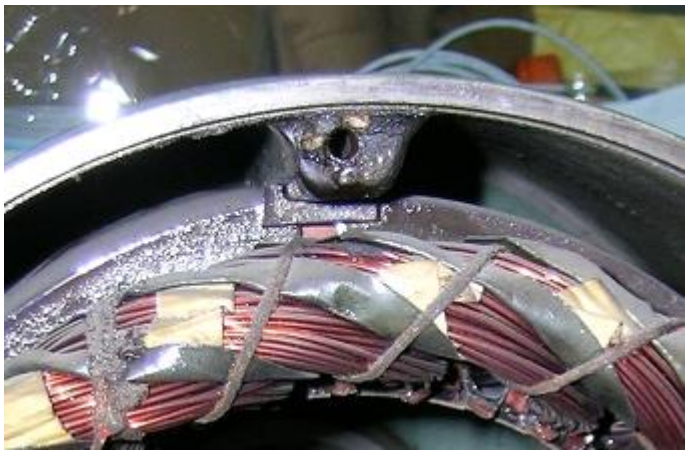

Fig. 6: One of the twelve stator core supports of the stator core.

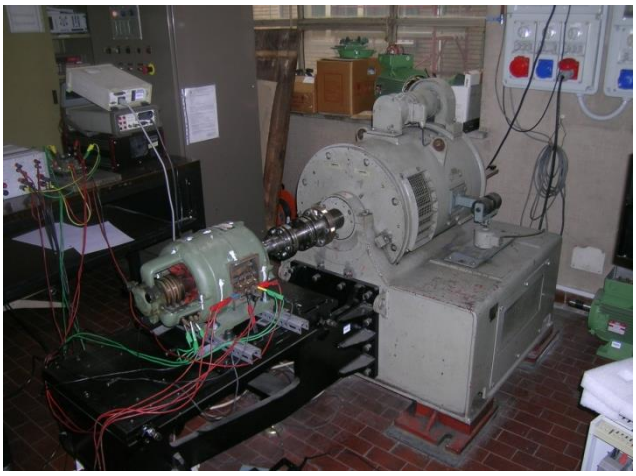

Fig.7: Load test set up

In order to understand if the value of the equivalent interface gap could be considered reasonable, a computation of its value has been carried out using the established equations of heat transfer theory [14], [15]. The obtained results have shown that the value of 0.6 mm can be considered a reasonable value for the equivalent interface gap due to the air in the duct and the stator lamination supports.

IV. LOAD TEST AND THERMAL MODEL VALIDATION.

The proposed thermal model has been validated comparing the computed and measured temperatures in load conditions.
The machine has been tested in load condition in accordance to the IEEE Std.112 - method B. The machine has been tested in no-load and locked rotor condition for the computation of the machine equivalent circuit parameters and the segregation of the no-load losses. The motor has been loaded using a dynamometer DC generator. The test bench and its set up is shown in Fig. 7. Table II shows the machine losses obtained

from the motor tests, where the mechanical losses and the additional losses have been included in the rotor joule losses.

TABLE II
MOTOR LOSSES AT RATED LOAD

Iron Losses [W]	Stator joule losses [W]	Rotor Joule losses [W]
141.7	214.2	241.1

During the load test, a cooling forced air flows inside the machine and its effect has to be considered in the thermal model.
In Total Enclosed Fan Cooled "TEFC" induction motors the cooling forced air flows on the motor finned frame surface. As discussed in [7] its thermal behavior can be represented by a thermal resistance in parallel to the natural convection thermal resistance (see Fig. 3). In the machine under test the cooling forced air does not flow on the motor frame outer surface, but its flows inside the machine. For this reasons, the forced air thermal resistance $R_{F\text{-}Conv}$ previously mentioned has been neglected assuming for it a very high value. On the other hand, the cooling effect of the cooling forced air has to be correctly included in the thermal model. The complexity of the cooling forced air system an approach based on the introduction of cooling power generators in the thermal network has been used. This solution is not new because its follows approaches used on commercial programs for electrical machine thermal analysis [16].
The following three cooling power generators have been included in the thermal model: $P_{ir\text{-}FR\text{-}Cool}$, $P_{EW\text{-}Cool}$ and $P_{AG\text{-}Cool}$.
The cooling power generator $P_{ir\text{-}FR\text{-}Cool}$ takes into account the forced air flowing inside the duct between the stator lamination and the machine frame. The value of this generator has been computed assuming the interface gap between the stator lamination and the frame as a channel with annular section, having the external diameter equal to the frame inner diameter, the inner diameter equal to the lamination outer diameter and a length equal to the stator core length. By the thermal equation for an annular section duct (11), the cooling power can be calculated.

$$P_{Ir-FR-Cool} = h_m \cdot (T_{Ir} - T_m) \cdot \pi \cdot l_{St} \cdot D_{S\_out} \tag{11}$$

Where h_m can be calculated by (12)

$$h_m = \frac{Nu \cdot k_{Air}}{d_{eq}} \tag{12}$$

and

$$Nu = 0{,}023 \cdot Re^{0,8} \cdot Pr^{0,4} \cdot \left(1 + \frac{d_{eq}}{l_c}\right)^{0,7} \tag{13}$$

$$Pr = \frac{c_{Air} \cdot \mu_{Air}}{k_{Air}} \tag{15}$$

$$Re = \frac{v_{Air} \cdot \rho_{Air} \cdot d_{eq}}{\mu_{Air}} \tag{15}$$

Fig. 8: Opening for the air speed measurement.

and with,

$$d_{eq} = \frac{D_{FR-i}^2 - D_{s-out}^2}{D_{s-out}} \tag{16}$$

The value of T_m can be calculated by (17).

$$T_m = \frac{T_{amb} + T_{ex-ec}}{2} \tag{17}$$

The measuring of the cooling air speed v_{air} inside the duct was possible via an opening in the machine frame at the opposite side of the terminal box (see Fig. 8), using a hot wire anemometer, while the lamination and air temperature were measured by a digital thermometer. Obviously this opening was sealed during the load tests. The value of the measured air speed at rated speed was 8.7 m/s.
The cooling power obtained by (11) was 110 W, with an average temperature of the cooling air of 31.8 °C
The cooling power generators $P_{EW\text{-}Cool}$ and $P_{AG\text{-}Cool}$ take into account the cooling forced air active inside the machine. In particular, $P_{EW\text{-}Cool}$ represents the air forced cooling effects on the stator and rotor end-winding, while $P_{AG\text{-}Cool}$ represents the air forced cooling effects in the machine air-gap providing a significant contribution to the stator and rotor wires cooling. As widely recognized, an accurate determination of the air flow and its cooling effects in these machine parts, requires a Computational Fluid Dynamic (CFD) approach. CFD solutions are based on extremely complex three dimensional models which require a huge amount of computational time and related costs. In addition, a CFD approach is not so flexible as a specific model for a machine is required. As a consequence, in this analysis the authors have used a pragmatic approach in order to determine the values of the cooling generators $P_{EW\text{-}Cool}$ and $P_{AG\text{-}Cool}$.

Let's define P_{losses} the addition of the machine losses reported in Table II. The heat balances (18) and (19) of the machine under test have to be verified in steady state conditions.

$$P_{Forced-Cool} = P_{Losses} - P_{FR-AMB} \quad (18)$$

$$P_{Forced-Cool} = P_{Ir-FR-Cool} + P_{EW-Cool} + P_{AG-Cool} \quad (19)$$

TABLE III
ESTIMATED COOLING SOURCE VALUES

P_{FR-AMB} [W]	$P_{Ir-FR-Cool}$ [W]	$P_{EW-Cool}$ [W]	$P_{AG-Cool}$ [W]
29	110	229	229

TABLE IV
COMPARISON BETWEEN MEASURED AND PREDICTED TEMPERATURES DURING THE RATED LOAD TEMPERATURE TEST

	T_{Frame} [°C]	$T_{Stator\ iron}$ [°C]	$T_{Stator\ winding}$ [°C]	$T_{Rotor\ winding}$ [°C]
Predicted	41,9	66,6	71,3	75,4
Measured	39,4	63,0	69,4	79,6
Error [%]	6.5	5.8	2.7	-5.3

In (18) the machine losses are known and the heat dissipated for natural convection, $P_{FR-AMB,}$ can be determined by (10), where all the quantities are measured during the load test. As a consequence, (19) allows the consideration of the cooling contributions of the forced air $P_{EW-Cool}$ and $P_{AG-Cool}$. It is important to highlight that in the machine under test the heat transfer between the frame and the ambient for natural convection cannot be neglected with respect to the forced convection effects. This is because the cooling forced air flows in the duct and not on the machine frame outer surface, as previously described and discussed.
Finally, the values of $P_{EW-Cool}$ and $P_{AG-Cool}$ can be reasonable calculated by dividing by two the value given by (20)

$$P_{EW-Cool} + P_{AG-Cool} = P_{Forced-Cool} - P_{Ir-FR-Cool} \quad (20)$$

In Table III the value of all the forced air cooling powers are reported
Using the values reported in Table II and the obtained cooling power values, the machine temperature at rated load has been predicted and compared with the measured ones. Table IV shows the comparison between the measured and the predicted temperatures. The percentage of errors included in the same table is lower than 7% for all the more significant temperatures. It is an authors' opinion that the obtained results can be considered good in absolute, taking into account the complexity of the system under analysis.

V. FINAL REMARKS

As reported in the previous section, the proposed thermal model allows a more than reasonable prediction of the machines temperatures. Nevertheless, a critical approach to the model and an honest analysis of its limits must be properly reported.

In order to realize n simple and '*friendly*' thermal model, the choice of a lumped parameters thermal network with a limited number of components is mandatory, partly because the use of thermal models with a high number of components does not always guarantee better results. In fact, the reliable computation of several thermal resistances is not an easy task as discussed by the authors in [4] and [5]. The proposed thermal model considers a symmetrical machine from the longitudinal point of view (along the machine shaft), both for conventional TEFC motors and machines with internal ventilation. This approximation is questionable due to the forced air cooling flow produced by the fan mounted on one side of the shaft. As observed by the measured temperatures this asymmetry was put in evidence, but the difference between the right and left part of the machine can be reasonably neglected for a first simplified thermal analysis. The use of user-defined power generators for taking into account the forced air cooling could seem an overly simplified approach. However, as explained and discussed in the previous section, an accurate computation of the forced convection effects would require the use of CFD numerical tools. The proposed approach allows the prediction of the forced convection cooling power requested for maintaining the machines temperatures beneath the requested limits. Effective design of the cooling system is usually outside the competence of the electromagnetic designer.

VI. CONCLUSION

In this paper a simplified thermal model for wound rotor induction machines is presented. The model has been discussed and commented upon. The equations for the thermal resistance computation have been provided and verified by experimental tests. The procedure for performing the experimental tests for the thermal model set-up have been described and discussed. Finally, the validity of the proposed thermal model has been proved by means of the rated load temperature test, comparing the measured and the predicted temperature in the most critical parts of the machine. The agreement between experimental and simulation results are more than satisfying considering the complexity of the machine under analysis and the forced air cooling system utilised.

REFERENCES

[1] Available on http://www.gwec.net
[2] I. Boldea, F Blaabjerg, D. I. Klumpner. I. Serban, "Sensorless control of wound rotor induction generator (WRIG) for wind power", 37th IEEE Power Electronics Specialists Conference, 2006.
[3] H. Li, Z. Chen "Overview of different wind generator systems and their comparisons", IET Renew. Power Gener., 2008, Vol. 2, No. 2, pp. 123–138.
[4] D. Staton, A. Boglietti, A. Cavagnino, "Solving the More Difficult Aspects of Electric Motor Thermal Analysis, in small and medium size industrial induction motors", *IEEE Transaction on Energy Conversio*n, Vol.20 (3) pp.620-628.
[5] A. Boglietti, A. Cavagnino, D. Staton, "TEFC Induction Thermal Models: A Parameters Sensitivity Analysis", *IEEE Transactions*

on Industry Applications, Volume 41, Issue 3, May-June 2005, pp. 756 – 763.

[6] D. A. Staton, A. Cavagnino, "Convection Heat Transfer and Flow Calculations Suitable for Electric Machines Thermal Models", Transactions on Industrial Electronics, Special Session on Thermal Issues in Electrical Machines and Drives, Vol. 55, No. 10, October 2008, pp. 3509-3516.

[7] A. Boglietti, A. Cavagnino, M. Lazzari, and M. Pastorelli, "A simplified thermal model for variable-speed self-cooled industrial induction motor," *IEEE Transaction on Industry Applications*, vol. 39, no. 4, Jul./Aug. 2003, pp. 945–952.

[8] A. Boglietti, A. Cavagnino, "Analysis of the Endwinding Cooling Effects in TEFC Induction Motors", *IEEE Transactions on Industry Applications*, Vol. 43, No. 5, Sept.-Oct. 2007, pp.1214 – 1222.

[9] A. Boglietti, A. Cavagnino, M. Parvis, A. Vallan, "Evaluation of radiation thermal resistances in industrial motors", *IEEE Transactions on Industry Applications*, Vol. 42, No. 3, May/June 2006, pp. 688-693.

[10] N.Jaljal, J.-F. Trigeol, P. Lagonotte, "Reduced Thermal Model of an Induction Machine for Real-Time Thermal Monitoring", *IEEE Transactions on Industrial Electronics*, Vol. 55, No. 10, October 2008, pp.3535-3542.

[11] C. Kral, A. Haumer, T. Bauml, "Thermal Model and Behavior of a Totally-Enclosed-Water-Cooled Squirrel-Cage Induction Machine for Traction Applications", *IEEE Transactions on Industrial Electronics*, Vol. 55, No. 10, October 2008, pp.3555-3564.

[12] J. Mugglestone, S.J. Pickering, D. Lampard, "Effect of Geometry Changes on the Flow and Heat Transfer in the End Region of a TEFC Induction Motor", *9th IEE Intl. Conf. Electrical Machines & Drives*, Canterbury, UK, Sept 1999.

[13] C. Micallef, S.J. Pickering, K.A. Simmons, K.J. Bradley, "An Alternative Cooling Arrangement for the End Region of a Totally Enclosed Fan Cooled (TEFC) Induction Motor", *IEE Conf. Rec. PEMD* 08, 3-5 April 2008, York, UK.

[14] J.P. Holman, Heat Transfer, McGraw-Hill, 1997.

[15] A.F. Mills, Heat Transfer, Prentice Hall, 1999.

[16] www.motor-design.com